

## Supplementary Information (ESI) Soft Matter

### Assessing the Extent of Structural and Dynamic Modulation of Membrane Lipids due to Pore Forming Toxins: Insights from Molecular Dynamics Simulations

Vadhana Varadarajan<sup>a</sup>, Rajat Desikan<sup>a</sup> and K. G.  
Ayappa<sup>\*,a,b</sup>

---

<sup>0a</sup> *Department of Chemical Engineering, Indian Institute of Science, Bangalore-560012, India*

<sup>0b</sup> *Centre for BioSystems Science and Engineering, Indian Institute of Science, Bangalore-560012*

<sup>0\*</sup>Corresponding author: Fax: +91-80-2360-8121, Tel: +91-80-2293-2769, Email: ayappa@iisc.ac.in

Table S1: System Details for ClyA and AHL Molecular Dynamics Simulations

|  | ClyA                             | AHL                              |
|--|----------------------------------|----------------------------------|
| System size (number of atoms)                                | 526274                           | 435739                           |
| Simulation box size - L (nm) $\times$ W (nm) $\times$ H (nm) | 16.1 $\times$ 16.1 $\times$ 19.9 | 17.3 $\times$ 17.3 $\times$ 14.4 |
| Number of DMPC lipid molecules                               | 688                              | 877                              |
| Number of water molecules                                    | 128832                           | 99681                            |
| Run-times of simulations (ns)                                | 500                              | 500                              |
| Salt concentration (mM)                                      | 150                              | 150                              |
| Number of Na <sup>+</sup> ions                               | 623                              | 449                              |
| Number of Cl <sup>-</sup> ions                               | 539                              | 456                              |
| Temperature (K)  | 310                              | 310                              |
| Pressure (bar, semi-isotropic)                               | 1                                | 1                                |

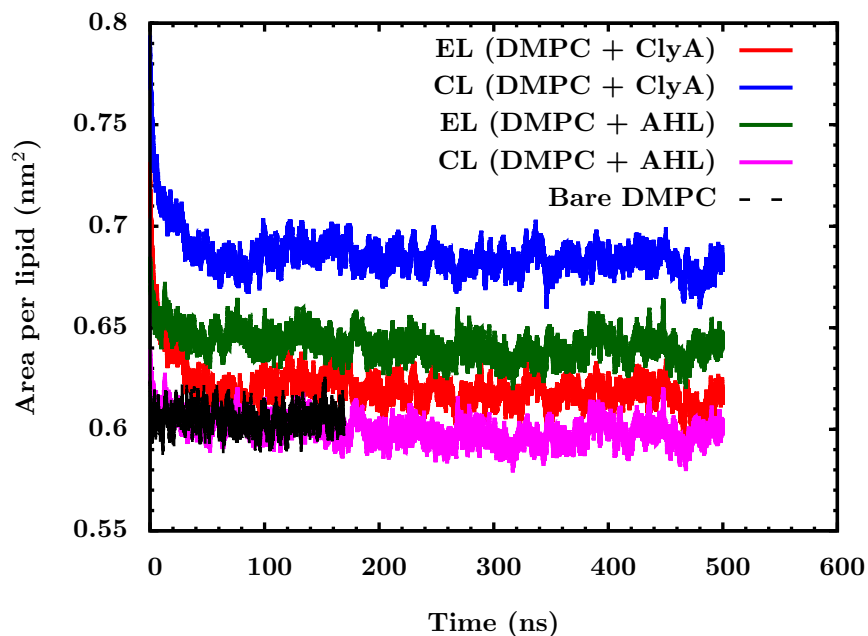


Figure S1: Area per lipid,  $a_l$ , for the PFT bound DMPC bilayer. The values of  $a_l$  indicate that areal fluctuations stabilize within the first 100 ns.

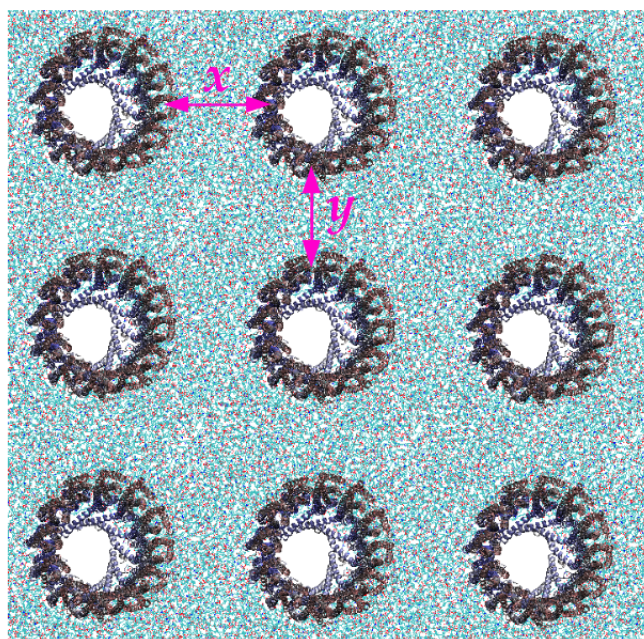


Figure S2: Periodic images of cytolysin A pores in the DMPC bilayer. The pores are separated at about 3.9 nm in the EL and 5.2 nm in the CL and are equidistant along the  $x$  and  $y$  directions.

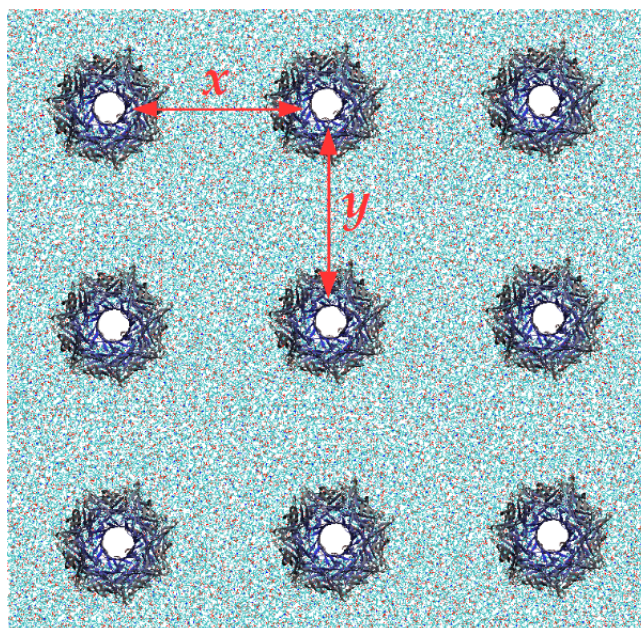


Figure S3: Periodic images of  $\alpha$ -Hemolysin pores in the lipid bilayer. The pores are 6.4 nm away in the the EL and 6.8 nm away in the CL and are equidistant along the  $x$  and  $y$  directions.

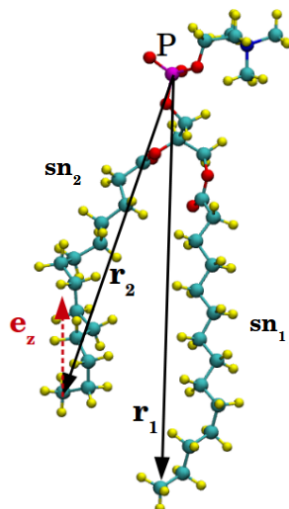


Figure S4: Illustration of the tilt angle subtended by the vector from the head group to the C-14 acyl carbon with the bilayer normal.

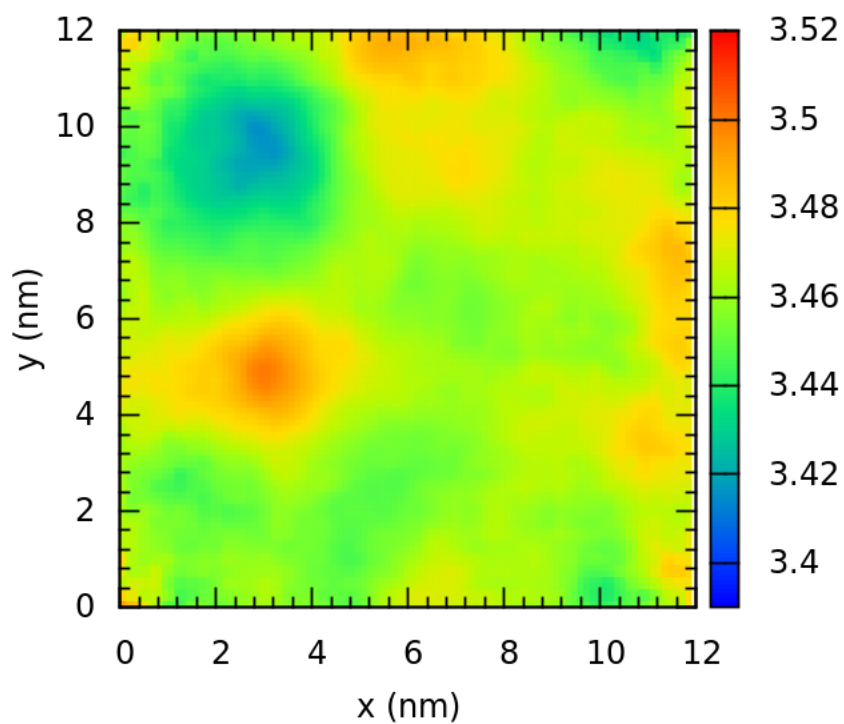


Figure S5: Thickness map of a bare DMPC bilayer at 310 K.

Table S2: Number of protein-membrane atomic contacts for the  $\alpha$ -hemolysin and cytolysin A pores. Values scaled to 100 with the maximum number of contacts are illustrated in Figures 11 & 13 of the main manuscript.

|                             | AHL                  | ClyA                 |
|-----------------------------|----------------------|----------------------|
| Protein-CL                  | 25136.0 $\pm$ 999.4  | 85391.3 $\pm$ 2133.8 |
| Protein-CL (headgroup)      | 6286.5 $\pm$ 480.1   | 15178.8 $\pm$ 965.6  |
| Protein-CL (sn1)            | 11249.5 $\pm$ 689.9  | 36114.9 $\pm$ 1086.0 |
| Protein-CL (sn2)            | 7600.0 $\pm$ 674.2   | 34097.6 $\pm$ 1520.1 |
| Protein-EL                  | 75643.0 $\pm$ 2055.8 | 75961.7 $\pm$ 1673.5 |
| Protein-EL (headgroup)      | 44191.5 $\pm$ 1284.3 | 18828.7 $\pm$ 910.6  |
| Protein-EL (sn1)            | 12667.0 $\pm$ 1047.5 | 25413.7 $\pm$ 1342.4 |
| Protein-EL (sn2)            | 18784.4 $\pm$ 928.3  | 31719.3 $\pm$ 1443.6 |
| Polar AA-CL                 | 5170.8 $\pm$ 359.7   | 13310.0 $\pm$ 565.8  |
| Polar AA-CL (headgroup)     | 2702.3 $\pm$ 283.1   | 2362.6 $\pm$ 401.8   |
| Polar AA-CL (sn1)           | 1532.8 $\pm$ 228.8   | 6158.3 $\pm$ 350.4   |
| Polar AA-CL (sn2)           | 935.7 $\pm$ 140.8    | 4789.1 $\pm$ 358.6   |
| Polar AA-EL                 | 37805.8 $\pm$ 1278.8 | 38686.3 $\pm$ 719.3  |
| Polar AA-EL (headgroup)     | 25330.2 $\pm$ 885.2  | 13743.1 $\pm$ 612.8  |
| Polar AA-EL (sn1)           | 4671.3 $\pm$ 523.8   | 10471.6 $\pm$ 612.4  |
| Polar AA-EL (sn2)           | 7804.3 $\pm$ 441.3   | 14471.7 $\pm$ 655.9  |
| Non-polar AA-CL             | 19965.2 $\pm$ 783.3  | 72081.3 $\pm$ 1773.6 |
| Non-polar AA-CL (headgroup) | 3584.2 $\pm$ 338.8   | 12816.1 $\pm$ 761.1  |
| Non-polar AA-CL (sn1)       | 9716.6 $\pm$ 552.4   | 29956.6 $\pm$ 1024.0 |
| Non-polar AA-CL (sn2)       | 6664.3 $\pm$ 574.7   | 29308.5 $\pm$ 1315.1 |
| Non-polar AA-EL             | 37837.2 $\pm$ 976.6  | 37275.4 $\pm$ 1326.4 |
| Non-polar AA-EL (headgroup) | 18861.3 $\pm$ 521.3  | 5085.6 $\pm$ 399.8   |
| Non-polar AA-EL (sn1)       | 7995.7 $\pm$ 694.7   | 14942.1 $\pm$ 967.9  |
| Non-polar AA-EL (sn2)       | 10980.1 $\pm$ 663.1  | 17247.6 $\pm$ 943.0  |
| RKWY-CL (headgroup)         | 828.1 $\pm$ 180.1    | 626.5 $\pm$ 129.9    |
| RKWY-CL (sn1 & sn2)         | 76.0 $\pm$ 32.3      | 8258.6 $\pm$ 365.6   |
| RKWY-EL (headgroup)         | 17048.5 $\pm$ 534.0  | 9261.4 $\pm$ 405.6   |
| RKWY-EL (sn1 & sn2)         | 4697.8 $\pm$ 216.1   | 19612.9 $\pm$ 607.9  |